33rd Annual International Conference of the IEEE EMBS
Boston, Massachusetts USA, August 30 - September 3, 2011

A Continuous, Wearable, and Wireless Heart Monitor using Head Ballistocardiogram (BCG) and Head Electrocardiogram (ECG)

David Da He, Eric S. Winokur, and Charles G. Sodini

Abstract— **Continuous and wearable heart monitoring is essential for early detection and diagnosis of cardiovascular diseases. We demonstrate a continuous, wearable, and wireless heart monitor that is worn at the ear. The device has the form factor of a hearing aid and is wirelessly connected to a PC for data recording and analysis. With the ear as an anchoring point, the heart monitor measures the ballistocardiographic (BCG) motion of the head using a MEMS tri-axial accelerometer, which is an electrode-less method to measure heart rate. Additionally, electrocardiogram (ECG) is measured locally near the ear using a single-lead configuration. The peak timing delay between the head ECG and the head BCG, or RJ interval, can be extracted in the presence of noise using cross-correlation. The RJ interval is shown to correlate to the heart's pre-ejection period during both Valsalva and whole-body tilt maneuvers.**

I. Introduction

CARDIOVASCULAR disease (CVD) affects 37% of the United States population and is the leading cause of death in the U.S. [1]. For the next twenty years, the medical cost of CVD is projected to triple from $273 billion to $818 billion due to the aging population [1]. To reduce this cost, the traditional hospital-centric healthcare system is shifting towards a consumer-oriented individual healthcare system [2]. This individual-centric paradigm emphasizes early detection and diagnosis [3].

Heart monitors that continuously measure heart rate, electrocardiogram (ECG), and heart intervals aid the early detection of risk factors by providing the long term data necessary for an accurate and timely diagnosis [4]. Currently, clinical continuous heart monitoring is usually performed using Holter monitors, which measure chest ECG using multiple leads. Single-lead continuous heart monitors have been demonstrated by works such as [5] [6] [7], all of which are located at the torso using chest or waist bands. As for consumer products, a popular continuous heart monitor is the wrist-watch heart rate monitor, which involves a chest strap that senses ECG [8].

We demonstrate a continuous, wearable, and wireless heart monitor that is worn at the ear in the form factor of a hearing aid. The ear location is chosen because the ear provides a natural anchoring point as proven by hearing aids and headsets [9]. The device monitors the heart using both mechanical and electrical methods. Mechanically, the device detects the head's ballistocardiographic (BCG) motion due to the heart's pumping of blood. This head BCG signal allows the measurement of heart rate. Electrically, the device measures ECG near the ear, which also yields heart rate. When combined, the BCG and ECG signals yield additional timing information about heart intervals.

Manuscript received March 26, 2011. This work was supported in part by the MIT Center for Integrated Circuits and Systems and by the Canadian NSERC Scholarship.

D. He, E.S. Winokur, and C.G. Sodini are with the Department of Electrical Engineering and Computer Science, Massachusetts Institute of Technology, Cambridge, MA, 02139 USA (e-mail: davidhe@mit.edu, ewinokur@mit.edu, sodini@mtl.mit.edu)

II. Measuring Head Ballistocardiogram

The ballistocardiogram (BCG) is a measure of the body's mechanical reaction to the blood ejected during systole. BCG is traditionally measured by having the subject lie on a low-friction bed [10]. The displacement of the bed is then captured as BCG. Alternative methods using pneumatic chair and strain-sensing foot scale have also proven successful [11] [12]. However, all of the above methods involve a large stationary BCG measurement device. Meanwhile, it has been documented in the MRI society that ballistocardiographic head movements are a source of movement artifacts in MRI [13]. Therefore, we can achieve a proxy measurement of BCG by sensing head movements instead of sensing the body movements. Because the neck is flexible, the morphology of the head BCG will differ from that of the traditional BCG.

To sense the head's BCG movements in a portable and wearable manner, we use a MEMS tri-axial accelerometer that is mounted at the ear. Because the BCG acceleration of the head is in the range of mG's, a highly sensitive and low noise accelerometer is required. Bosch's BMA180 is chosen for its 14-bit resolution and 0.69mG$_{RMS}$ of measured noise at 10Hz bandwidth with $\pm$2G range. Because BCG records acceleration, any major motion such as walking will overwhelm the low-amplitude BCG signal. Therefore, head BCG is a measurement taken at rest (tolerated head motions include light chewing and speaking).

The advantage of this measurement is that it is electrodeless and wearable. Fig. 1 shows a measurement of head BCG in the upright standing posture. Here, the axis with the best BCG signal is the y-axis, or the up-down direction. This is consistent with the direction of blood volume shift. Additionally, it is seen that the head BCG acceleration is in the range of 10mG$_{p-p}$.

III. Measuring Head Electrocardiogram

Because the body is a conductive medium, the ECG signal from the heart can be detected elsewhere on the body in an attenuated form. Since the monitor is worn at the ear, we choose the mastoid area behind the ear to sense ECG, where

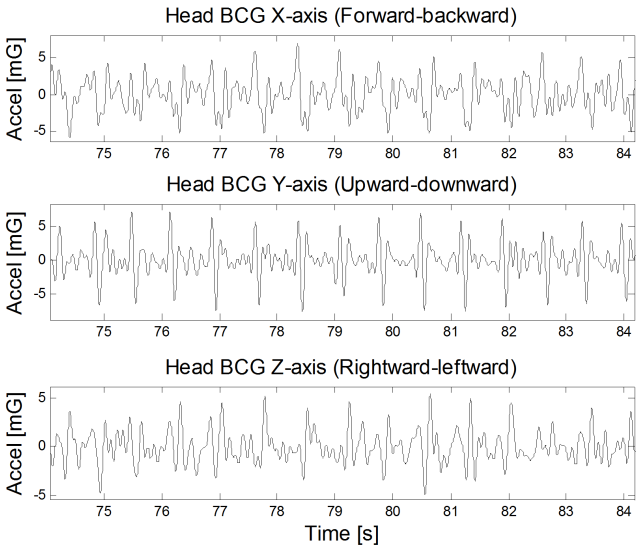

Fig. 1. A sample head BCG measurement taken while standing upright. The data is filtered with a 1-10Hz bandpass filter.

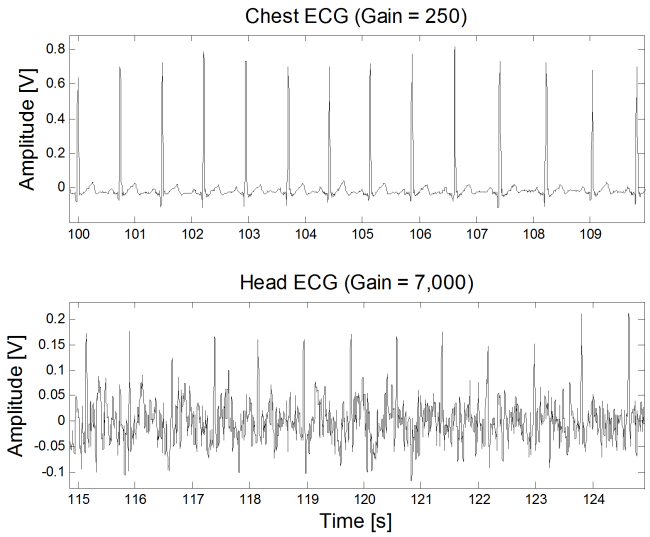

Fig. 3. Top: ECG measured from the chest. Bottom: ECG measured from the mastoid area behind the left ear. The ECGs are filtered with a 1-50Hz bandpass filter. Measurements are not simultaneous.

the bony structure and flat surface allow a stable electrode contact with minimal motion artifacts.

The head ECG front-end circuit is shown in Fig. 2. The circuit is kept as simple as possible to reduce component count and PCB area.

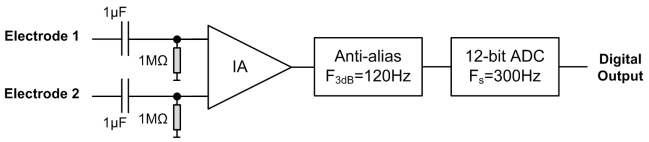

Fig. 2. The head ECG front-end circuit.

In Fig. 2, the two differential electrodes go through a high pass filter with a corner frequency of 0.16Hz. Then, the filtered differential signal is amplified by an instrumentation amplifier (IA) (Texas Instruments INA333) with an adjustable gain. The amplifier output is connected to a 12-bit SAR ADC (Analog Devices AD7466) with a sampling frequency of 300Hz. Because the ECG amplitude near the ear is in the range of μV's, the IA's noise performance is important. We choose INA333 for its low input-referred noise, which is comparable to the thermal noise generated by the 1MΩ biasing resistors within a bandwidth of 150Hz ($1.6\mu V_{RMS}$).

Common-mode feedback (CMFB) is usually used in ECG front-end circuits to reduce powerline interference and to set the DC level of the circuit. However, CMFB is not needed in this application because powerline interference is reduced by digital filtering. Also, the circuit's DC level is isolated by the high pass filters. This filtering removes the need for a CMFB electrode and eliminates its footprint.

Using clinical AgCl electrodes, Fig. 3 shows ECG measurements taken from the chest (lead II, 15cm apart, gain of 250) and from the left mastoid area (4cm apart, gain of 7,000, positioning is shown in Fig. 5).

As can be calculated from Fig. 3, the ECG measured at the mastoid area is in the range of 30-40μV_{p-p}, which is two orders of magnitude smaller than the chest ECG. This attenuation is due to the longer distance from the heart and the shorter distance between the differential electrodes. Because of the attenuation, the head ECG has a poor signal-to-noise ratio and is only measurable with minimal head motions. A robust method to extract information from the head ECG in the presence of noise will be discussed in Section V.

IV. System Description

The system consists of the BCG accelerometer, the ECG front-end, a power management circuit, a microcontroller, a wireless transmitter and receiver, the PC software, and the mechanical housing. Fig. 4 shows the system block diagram.

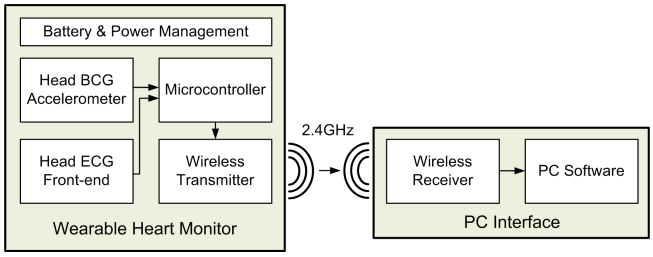

Fig. 4. The system block diagram with arrows indicating the signal path.

The BCG and ECG components have been described in Sections II and III. The power management circuit is supplied by a 3V lithium coin cell battery (Panasonic CR2032) and consists of a DC-DC converter and a linear regulator. To reduce power supply noise for the analog front-end, the digital circuits are powered from the DC-DC converter, and the analog circuits are powered from the linear regulator.

The microcontroller (Texas Instruments MSP430) shuttles continuous real time BCG and ECG data to the 2.4GHz low-power wireless transmitter (Texas Instruments CC2500). Wireless data is sent to a wireless receiver (CC2500) using the open source low-power SimpliciTI protocol. The receiver communicates with a PC via a custom-made UART-to-USB dongle. The PC records, plots, and analyzes the BCG and ECG data in real time using MATLAB.

The mechanical housing of the wearable device is modified from a hearing aid housing. Fig. 5 shows the entire system and shows the device being anchored to the ear similar to a hearing aid.

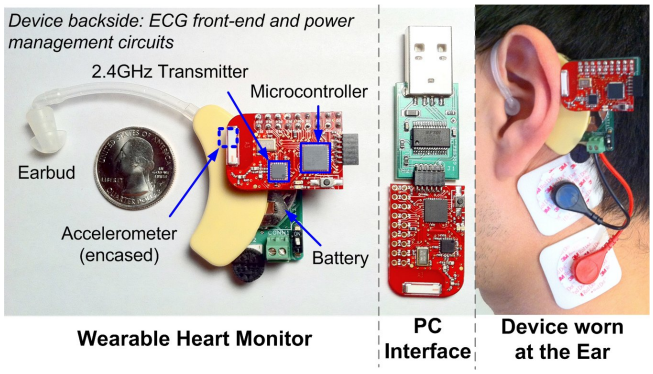

Fig. 5. The wearable heart monitor, the PC USB interface, and the heart monitor being worn at the ear with ECG electrodes attached.

V. Determining the RJ Interval using Cross-correlation

The RJ interval is the electromechanical delay between the left ventricular depolarization (ECG's R wave) and when the body experiences the greatest recoil from pumped blood (BCG's J wave) [14] [15]. The RJ interval is of physiological significance because it has been shown to correlate with the pre-ejection period (PEP), which relates to the heart's contractility and can be used to diagnose certain heart diseases [15] [16] [17].

To measure the RJ interval, the simplest method is to use a peak detection algorithm to determine the delay between the ECG peak and the BCG peak. However, as shown in Fig. 1 and Fig. 3, head BCG and head ECG have inherently weak signals. Here, a peak detection algorithm could easily misinterpret noise as a peak. Therefore, a noise-tolerant method is needed for RJ interval calculation.

We propose cross-correlation as a robust method for determining the RJ interval. This method takes advantage of the fact that both head BCG and head ECG waveforms have a similar morphology and are phase-locked. To determine the RJ interval, a time window of the head ECG signal is cross-correlated with the same time window of the head BCG signal. The result of such a correlation is shown in Fig. 6.

In Fig. 6, the highest peak of the cross-correlation occurs when the R wave of ECG and the J wave of BCG coincide during shifting. The lag index of the highest cross-correlation peak is thus the RJ interval. To shorten calculations, the

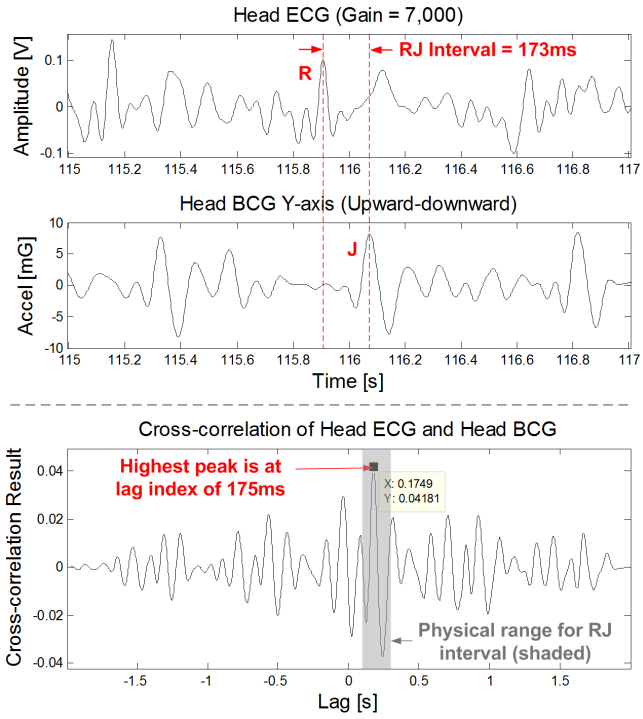

Fig. 6. A two-second time window of head ECG and head BCG are cross-correlated (both bandpassed filtered 1-20Hz). The lag index of the highest peak in the cross-correlation is the RJ interval.

cross-correlation can be limited to a lag range of 0.1s to 0.3s because RJ intervals physically fall in this range [12]. Further noise tolerance can be achieved by increasing the length of the time window of BCG and ECG. This uses more R and J waves to calculate the correct correlation, albeit at the cost of losing high frequency features of the RJ interval. In our testing, a three-second time window is sufficient to reliably extract RJ intervals compared to manual extraction.

VI. Changes in RJ Interval due to Hemodynamic Responses

Fig. 7 shows the RJ interval measured during a Valsalva maneuver performed in the sitting posture. PEP was simultaneously measured using a Sonosite BioZ Dx impedance cardiography (ICG) machine. Here, the RJ interval is shown to correlate to the PEP. In particular, during the strain, ventricular filling volume is reduced, which leads to a prolonged PEP [17] [18]. The PEP's increase of 30ms correlates to an equal increase in RJ interval as seen between 62s and 83s. Then, as the sustained strain lowers the blood pressure, the baroreceptor reflex activates the sympathetic response, and PEP begins to shorten due to increased heart contractility [18]. This corresponds to the drop in PEP and RJ interval just before the release. The results in Fig. 7 are consistent with the RJ interval trends during Valsalva and with the PEP correlation documented in [15] and [16].

Fig. 8 shows simultaneously measured RJ interval and PEP during a whole-body tilt test. As the body is tilted from 0° (supine) to 80° (tilt), an increase in RJ interval is observed. This correlates to the observed increase in PEP in the tilted

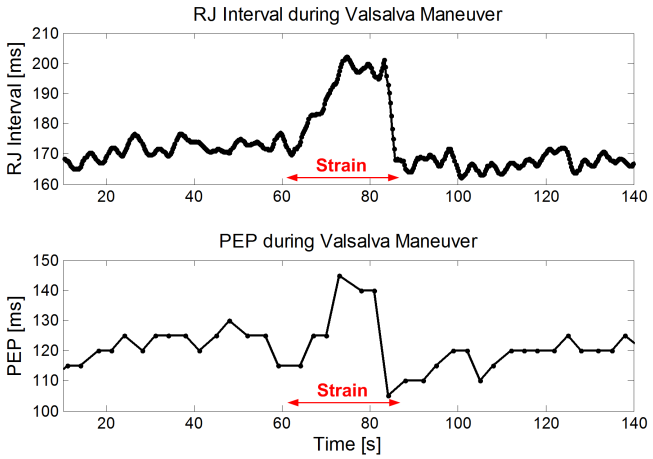

Fig. 7. Simultaneously measured RJ interval and PEP during a Valsalva maneuver. The PEP is measured using thorax-neck ICG sampled at 200Hz.

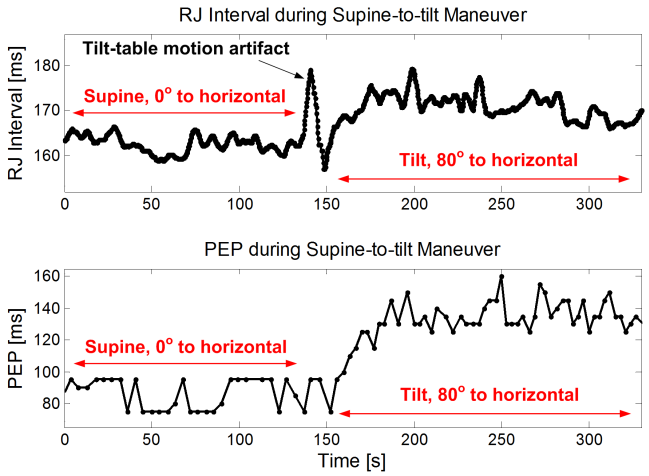

Fig. 8. Simultaneously measured RJ interval and PEP during a whole-body tilt test. The PEP is measured using thorax-neck ICG sampled at 200Hz.

position, which is caused by the reduction of ventricular filling volume [17] [18]. However, PEP increases by 45ms while RJ interval only increases by 15ms. We hypothesize this to be due to the change in head BCG's morphology in the supine position, where the head movement is impeded by frictional contact with the bed and the RJ interval is mechanically prolonged.

VII. Conclusions and Future Work

In summary, a continuous and wearable heart monitor at the ear has been demonstrated. Using the ear as a natural anchor, the device measures head BCG and head ECG, each of which yields the heart rate. The RJ interval between the measured ECG and BCG signals can be calculated in the presence of noise using cross-correlation. The RJ interval is shown to correlate to PEP during the Valsalva maneuver and the whole-body tilt test.

In its current implementation, the system sends continuous real time data wirelessly to the PC for analysis. A future implementation will perform the analysis on the microcontroller and periodically send scalar data such as heart rate and RJ interval to the PC. This will drastically reduce the radio's duty cycle and power consumption (20mA transmission current). Furthermore, significant size reduction of the device is possible by combining the microcontroller/radio daughterboard with the motherboard and by integrating the discrete ECG front-end components into an integrated circuit.

VIII. Acknowledgments

The authors would like to thank Dr. Thomas Heldt for his valuable discussions and his experimental assistance.

References

[1] P. Heidenreich et al., "Forecasting the future of cardiovascular disease in the United States: a policy statement from the American Heart Association," *Circulation*, vol. 123, pp. 933-944, 2011.

[2] G. Troster, "The agenda of wearable healthcare," *IMIA Yearbook of Med. Info. 2005: Ubiquitous Health Care Sys.*, pp. 125-138, 2004.

[3] X.-F. Teng, Y.-T. Zhang, C.C.Y. Poon, and P. Bonato, "Wearable medical systems for p-health," *IEEE Reviews in Biomedical Engineering*, vol. 1, pp. 62-74, 2008.

[4] A. Lymberis, "Smart wearable systems for personalised health management: current and and future challenges," *IEEE Eng. Med. Biology Conf.*, pp. 3716-3719, 2003.

[5] J. Muhlsteff et al., "Wearable approach for continuous ECG - and activity patient-monitoring," *IEEE Eng. Med. Biology Conf.*, pp. 2184-2187, 2004.

[6] J. Yoo et al., "A 5.2mW self-configured wearable body sensor network controller and a 12W 54.9% efficiency wirelessly powered sensor for continuous health monitoring system," *International Solid-State Circuits Conference*, pp. 290-291, 2009.

[7] C. Park, P.H. Chou, B. Ying, R. Matthews, and A. Hibbs, "An ultra-wearable, wireless, low power ECG monitoring system," *Biomedical Circuits and Systems Conference*, pp. 241-244, 2006.

[8] M. Kingsley, M.J. Lewis, and R.E. Marson, "Comparison of Polar 810s and an ambulatory ECG system for RR interval measurement during progressive exercise," *Intl. J. Sports Med.*, vol. 26, pp. 39-44, 2005.

[9] D. He, E. Winokur, T. Heldt, and C. Sodini, "The ear as a location for wearable vital signs monitoring," *IEEE Eng. Med. Biology Conf.*, pp. 6389-6392, 2010.

[10] I. Starr, A.J. Rawson, H.A. Schroeder, and N.R. Joseph, "Studies on the estimation of cardiac output in man, and of abnormalities in cardiac function, from the heart's recoil and the blood's impacts; the ballistocardiogram," *The American Journal of Physiology*, vol. 127, pp. 1-28, 1939.

[11] K.K. Kim et al., "A new method for unconstrained pulse arrival time measurement on a chair," *J. Biomed. Eng. Res.*, vol. 27, pp. 83-88, 2006.

[12] O.T. Inan, M. Etemadi, R.M. Wiard, L. Giovangrandi, and G.T.A. Kovacs, "Robust ballistocardiogram acquisition for home monitoring," *Physiological Measurement*, vol. 30, pp. 169-185, 2009.

[13] G. Bonmassar et al., "Motion and ballistocardiogram artifact removal for interleaved recording of EEG and EPs during MRI," *NeuroImage*, vol. 16, pp. 1127-1141, 2001.

[14] J.H. Shin, K.M. Lee, and K.S. Park, "Non-constrained monitoring of systolic blood pressure on a weighing scale," *Physiol. Meas.*, vol. 30, pp. 679-693, 2009.

[15] O.T. Inan, M. Etemadi, R.M. Wiard, G.T.A. Kovacs, and L. Giovangrandi, "Non-invasive measurement of Valsalva-induced hemodynamic changes on a bathroom scale ballistocardiograph," *IEEE Eng. Med. Biology Conf.*, pp. 674-677, 2008.

[16] M. Etemadi, O.T. Inan, R.M. Wiard, G.T.A. Kovacs, and L. Giovangrandi, "Non-Invasive assessment of cardiac contractility on a weighing scale," *IEEE Eng. Med. Biology Conf.*, pp. 6773-6776, 2009.

[17] R.W. Stafford, W.S. Harris, and A.M. Weissler, "Left ventricular systolic time intervals as indices of postural circulatory stress in man," *Circulation*, vol. 41, pp. 485-492, 1970.

[18] V.V. Ermishkin et al., "Beat-by-beat changes in pre-ejection period during functional tests evaluated by impedance aortography: a step to a left ventricular contractility monitoring," *Intl. Conference on Electrical Bioimpedance*, vol. 17, pp. 655-658, 2007.